LAWRENCE
LIVERMORE
NATIONAL
LABORATORY

UCRL-JRNL-201881

# Structure, Vibrational and Electronic Spectra of Heterofullerene C48(BN)6

M. R. Manaa, R-H. Xie, V. H. Smith, Jr.

January 16, 2004

Chemical Physics Letters

# Structure, vibrational and electronic spectra of heterofullerene $C_{48}(BN)_6$

M. Riad Manaa [1*], Rui-Hua Xie [2†] and Vedene H. Smith, Jr. [2]

[1] University of California, Lawrence Livermore National Laboratory, Energetic Materials Center, L-282, Livermore, California, 94551, USA

[2] Department of Chemistry, Queen's University, Kingston, ON K7L 3N6, Canada

[*] Corresponding author. Email: manaa1@llnl.gov

[†] Present address: NIST, Gaithersburg, MD 20899-8423, USA.

To be submitted to Chemical Physics Letters

**Abstract:**

We report the geometrical structure, vibrational, and excitation spectra of novel, fullerene – analog $C_{48}(BN)_6$ using density functional calculations. The lowest energy structure is one in which B-N bonding is present as boron and nitrogen occupy each of the twelve pentagons of the fullerene cage. The cluster is polar with a net dipole moment of 0.55 Debye, which indicates an enhanced tendency toward reactivity with other media. The excitation spectrum shows that the lowest transition of 1.75 eV is dipole-allowed. The optical gap of $C_{48}(BN)_6$ is redshifted by 1.17 eV relative to that of $C_{60}$, suggesting possible use as single-molecule fluorescent probes for various applications.

The inclusion of dopants, such as nitrogen or boron, in the $C_{60}$ shell is an attractive avenue to manipulate the electronic, optical, and magnetic properties of fullerenes and make the resulting clusters candidates for interesting applications. Both dopents have so far been within the experimental realm: the formation of molecular species of the type $C_{60-2n}$ $N_{2n}$ was obtained by contact-arc vaporization of graphite in the presence of pyrrole, [1] and a series with the stoichiometry $C_{60-n}$ $B_n$ ($1 \leq n \leq 6$) was also created.[2] In a more recent report, the production of cross-linked nano-onions that correspond to a core shell of $C_{48}N_{12}$ was achieved through reactive sputtering of graphite in $N_2$. [3] The molecular geometry,[4] vibrational, [5] and electronic properties [6,7] of the ground state structure, its condensed fcc electronic structure aspects, [8] and properties of several related isomers were computationally elucidated. [5, 7, 9-12] Compared to $C_{60}$, $C_{48}N_{12}$ showed an enhancement of its second hyperpolarizibility by about 55%, making it a good candidate for optical limiting applications. [11] It was also shown that $C_{48}N_{12}$ could be used to build diamagnetic materials due to its enhanced diamagnetic shielding factor in the carbon atom. [10] Moreover, electron acceptor $C_{48}B_{12}$ and donor $C_{48}N_{12}$ have been shown to be promising components for molecular rectifiers, carbon nanotube-based *n-p-n* (*p-n-p*) transistors and *p-n* junctions. [13, 14]

In this study, we report calculations on the fullerene-analog in which both nitrogen and boron dopants are present, that of $C_{48}B_6N_6$. The inclusion of both dopants is tempting since a boron nitride unit (BN) is isoelectronic with $C_2$, and boron nitride exists in both the hexagonal [15] and cubic [16] phases that are similar to the commonly known graphite and diamond phases of carbon, and have such desirable properties as extreme hardness (scratching diamond!), low dielectric constant, and high thermal stability.

Further, the inclusion of both dopants in the composition that synthesis has shown to be the most stable in the case of $C_{48}N_{12}$ [3] is most promising for experimental realization with rich optical properties and reactivity. Our reported results of the molecular geometry, harmonic vibrational frequencies, IR and Raman spectra are based on the B3LYP/6-31G* level of theory.[17, 18] This level of treatment was shown to be in remarkable agreement with higher ab initio methods such as MP2 and couple cluster with single and double excitation (CCSD) for the cubic clusters $B_4N_4$ and $C_8$.[19] The optical absorption spectrum is reported using time-dependent BP86/3-21G, which was shown to provide better electronic excitation spectra when compared with experiments. [7, 11]

We considered several molecular structures of $C_{48}B_6N_6$ that are thought to be the most energetically stable ones based on previous work of $C_{48}N_{12}$ and $C_{48}B_{12}$.[4, 20] The ground state molecular structure of $C_{48}N_{12}$ includes two triphenylene-type units (four all-carbon hexagons) that constitute the top and bottom portion of the buckyball as shown in Fig.1. Three nitrogen atoms are included within each of these units, one atom per pentagon. The remaining six nitrogen atoms are distributed around the equator of the cage structure within the remaining six pentagons; each atom is separated from its neighboring kind of the tiphenylene unit by a carbon atom. The extended region of electron delocalization in the tiphenylene units enhances the molecular stability via resonance energy contributions, while precluding a weaker N-N link. The structure was shown to be about 0.5 eV more stable than an earlier isomer with only two all-carbon hexagons, but with nitrogen atoms being separated by at least two carbon atoms.[9] Recently, the extended aromatic stability of this same structure was also found to persist for the analogues $C_{48}B_{12}$, [20] and $C_{48}X_{12}$ (X= B, P, Si). [21] We thus chose four

structures for $C_{48}B_6N_6$ with the following B and N distributions: (1) B and N are bonded in each of the twelve pentagons (Fig.2), (2) nitrogen atoms are in the tiphenylene units while boron atoms are along the equator (Fig.1), (3) boron atoms are in the tiphenylene units while nitrogen atoms are along the equator (Fig.1), and (4) A structure based on Strafstrom's $C_{48}N_{12}$ structure that has only two all-carbon hexagons.

Table I lists the total and relative energies of the four isomers described above. We find that isomer 1, whose optimized geometry is shown in Fig.2, to be the most stable structure. Isomer 2 and 3 are 155.2 and 167.2 kcal/mol energetically less stable, respectively. All three structures have extended electron delocalization arising from the existence of eight, all-carbon, and benzene-like rings. Isomer 1, however, contains the six BN-bonded units, and will be referred to hereafter as $C_{48}(BN)_6$. The B-N bond is stronger than its counterparts, B-C and C-N bonds. This can be understood based on the fact that the boron is $sp^2$ hybridized, while nitrogen is purely *p*-orbital bonded, thus the B-N bond is a $sp^2$-*p* type. In isomer 2 and 3, the B-C and C-N bonds are of the type $sp^2$-$sp^3$ and $sp^3$-*p*, respectively. Along with the decreased resonance energy contribution, isomer 4 is the least stable with 186.5 kcal/mol relative to isomer 1.

Structurally, the bond distances in $C_{48}(BN)_6$ are similar to what was found in $C_{48}B_{12}$ and $C_{48}N_{12}$. Several carbon-carbon bonds exist ranging in length from 1.39Å to 1.49 Å. The various B-C bonds are calculated to be within the range of 1.53-1.55 Å, and the C-N bonds are either 1.42 or 1.43 Å. The B-N bond distance is found to be 1.44 Å, which is approximately a middle value between 1.36 Å and 1.50 Å found for the Planar (double bond character) [22] and the cubic (purely single) [19] $B_4N_4$, respectively.

Mulliken charge analysis of $C_{48}(BN)_6$ showed that twelve carbon atoms have positive charges in the range 0.19-0.22 $|q_e|$, while the remaining thirty-six atoms have negative charges between –0.08 and –0.01$|q_e|$. The six boron atoms have positive net charges of 0.27 and 0.28 $|q_e|$, and the six nitrogen atoms have a negative net charges of –0.49$|q_e|$. The nitrogen atoms can thus be considered as sites of electron acceptors, while the boron atoms as electron donors. The charges on both sites can be contrasted with those found in $C_{48}B_{12}$ and $C_{48}N_{12}$. In $C_{48}B_{12}$, we determined two types of boron atoms with net charges of 0.16 and 0.17 $|q_e|$,[20] while for $C_{48}N_{12}$ we reported the two types of nitrogen atoms to have negative net Mulliken charges of –0.59 $|q_e|$ and -0.60$|q_e|$.[4] Further, in contrast to $C_{60}$, $C_{48}B_{12}$ and $C_{48}N_{12}$, which have zero net dipole moment, $C_{48}(BN)_6$ is a polar cluster with a net dipole of 0.55 Debye. This polarity can thus have profound effects on the reactivity of this cluster with other media.

Table II lists the binding energy, ionization potential, and the HOMO-LUMO energies of $C_{48}(BN)_6$ and compare them with those of $C_{48}B_{12}$, $C_{48}N_{12}$, and $C_{60}$. The calculated binding energy of $C_{48}(BN)_6$ is 6.69 eV per atom, 0.29 eV/atom less than that of $C_{60}$, suggesting that the structure is amenable to synthesis. This value is 0.07 and 0.31 eV/atom larger than those of $C_{48}B_{12}$ and $C_{48}N_{12}$, respectively. As for the electronic properties, the calculated energy gap between the HOMO and LUMO molecular orbitals for $C_{48}(BN)_6$ is 2.72 eV, which is slightly lower than the corresponding gap for $C_{60}$, calculated to be 2.76 eV, and is in agreement with the experimental value of 2.3±0.1 eV of the solid phase. [23] In comparison, the $C_{48}(BN)_6$ energy gap is only 0.02 eV larger than that of $C_{48}N_{12}$, but significantly larger than that for $C_{48}B_{12}$ at 1.60 eV. It should be noted that both the HOMO and LUMO levels of $C_{48}(BN)_6$ are energetically higher than

that in $C_{60}$ by 0.27 and 0.24eV, respectively. This energetic ordering of the HOMO and LUMO levels accounts for the difference in the calculated first ionization potential of 6.92 eV, 0.32 eV lower than that of $C_{60}$.

Table III provides a list of the calculated harmonic vibrational frequencies and the infrared intensities of $C_{48}(BN)_6$. There are a total of 174 vibrational modes, forty-nine of which are classified as non-IR active, or having intensity less than 1 km/mol. This rich IR (and Raman) activity is primarily due to the low symmetry ($C_1$) of the cluster compared to $C_{60}$ ($I_h$) and $C_{48}N_{12}$ ($S_6$). We identify the strongest band to be associated with a frequency of 1599 $cm^{-1}$ and corresponding IR intensity of 53 km/mol. This band is identified to correspond with a C-C bond stretch. Similarly, the strongest bands were also identified in the case of $C_{48}N_{12}$ and $C_{48}B_{12}$ to occur at 1669 $cm^{-1}$ and 1490 $cm^{-1}$, respectively.[5, 20] The second strongest band, with intensity of 42 km/mol and associated with a frequency of 1532 $cm^{-1}$ is also identified to correspond mainly to a C-C bond stretch. Finally, the calculated zero-point energy of this cluster is 229.6 kcal/mol.

We also calculated the Raman-active vibrational frequencies of $C_{48}(BN)_6$, and the results are compared with those of $C_{60}$. For $C_{60}$, there are 10 Raman-active vibrational modes, 2 in $a_g$ modes (non-degenerate and fully polarized) and 8 in $h_g$ modes (fivefold-degenerate and unpolarized). In contrast with $C_{60}$, we find that there are a total of 174 independent Raman-active vibration modes because of the symmetry lowering which splits all degenerate vibrational modes observed in $C_{60}$ and makes many more modes Raman-active. These modes are classified in 16 unpolarized, 32 fully polarized and 126 incomplete polarized modes.

Here, we only calculate non-resonant Raman intensities. The results are shown in Fig.3. For $C_{60}$, the strongest Raman-active spectral lines, as shown in Fig.3, are the two non-degenerate $a_g$ modes.[12] Both modes are identified by their polarized character, which strongly suggests that they are totally symmetric. The remaining 8 Raman-active modes of $C_{60}$ are fivefold degenerate and unpolarized ones with $h_g$ symmetry.[12] The calculated results are in excellent agreement with experiment.[24]

In contrast, for $C_{48}(BN)_6$ we observe 16 unpolarized, 32 fully polarized, and 126 incomplete ploarized Raman spectroscopic signals. The Raman spectrum of $C_{48}(BN)_6$ separates into two regions, i.e., high-frequency (1100 $cm^{-1}$ to 1700 $cm^{-1}$) and low frequency (200 $cm^{-1}$ to 1000 $cm^{-1}$) regions, which are similar to those of $C_{60}$. The strongest Raman spectral lines in both low- and high-frequency regions are the fully polarized modes located at 1463 $cm^{-1}$ and 481 $cm^{-1}$, respectively, which are almost the same as those of the strongest $a_g$ modes of $C_{60}$. Six stronger Raman signals are located in the high-frequency region, i.e., at 1261, 1272, 1370, 1542, 1550, 1567 $cm^{-1}$ with $I_{raman}$=3.0, 4.2, 3.1, 3.8, 3.9, 3.3 (in unit of $10^{-12}$ $m^4/kg$), respectively. The weak Raman bands ($I_{raman} < 10^{-13}$) are observed mainly in the low-frequency region. As shown in Fig.3, the lowest and highest Raman-active frequencies of $C_{48}(BN)_6$ are almost the same as those of $C_{60}$.

The fullerene symmetry plays an important role in determining its optical activity such as the excitation and optical absorption spectra.[7] Over the past 10 years, many experimental and theoretical studies on the optical absorption of $C_{60}$ in the gas phase have been performed. Because of the $I_h$ symmetry of $C_{60}$, its LUMO (HOMO) has $t_{1u}$ ($h_u$) symmetry and thus its lowest singlet is dipole-forbidden (see Fig.4 (a)).[7] In the low-

energy excitations below 4.5 eV, as shown in Fig.4 (a), there appear only two dipole-allowed transitions (2.92 eV and 3.62 eV) located in the violet and ultraviolet regions, respectively.

As twelve carbon atoms in $C_{60}$ are substituted by six boron and six nitrogen atoms, the $I_h$ symmetry of changes to $C_1$. Correspondingly, as shown in Fig.5, the degeneracy of the ground-state levels, for example, the fivefold degenerate HOMO and the threefold degenerate LUMO, of $C_{60}$ is removed completely. Therefore, although it is an isoelectronic analogue to $C_{60}$, $C_{48}(BN)_6$ could exhibit richer features in the singlet excitation and absorption spectra than $C_{60}$. As shown in Fig.4 (b), the narrow singlet bands predicted for $C_{60}$ are split and expanded. In comparison, the lowest singlet (1.75 eV) for $C_{48}(BN)_6$ is dipole-allowed. Thus, the optical gap of $C_{48}(BN)_6$ appears in the red region, redshifted by 1.17 eV relative to that of $C_{60}$. In the visible region (<3.0 eV) reported in Fig.4 (b), the absorption spectrum of $C_{48}(BN)_6$ shows strong absorption in both blue and violet regions, but weak absorption in the red, orange, yellow and green regions. They are mainly from the excitation contributions of HOMO-*n* and LUMO+*n* pairs shown in Fig.5.

Since $C_{60}$ and $C_{48}(BN)_6$ differ in their optical gaps ranging from the violet to the red region, they may be used as single-molecule fluorescent probes for applications in polymer science, biology and medicine. Examples would be labeling DNA and RNA, lighting up polymers, photodynamic therapy, detection and identification of fullerrene-based drugs. Also, it is possible to develop $C_{60}$ - and $C_{48}(BN)_6$ -based fluorescent sensors and switches: (i) $C_{60}$ as a fluorophore module, responsible for both photonic transactions of excitation and emission; (ii) $C_{48}(BN)_6$ as a receptor module, responsible for guest

complexation and decomplexation; and (iii) a spacer module, responsible for holding the acceptor and donor close to, but separating from each other.[7] This kind of photoinduced electron-transfer signaling system has natural “on or off” switchability: it is the “on” (“off”) state if fluorescence is (not) observed in $C_{60}$.

**Acknowledgments:**

MRM work was performed under the auspices of the U.S. Department of Energy by the UC Lawrence Livermore National Laboratory under contract number W-7405-Eng-48. RHX would like to thank the HPCVL at Queen's University for the use of its parallel supercomputing facilities. VHS gratefully acknowledges the support from the Natural Science and Engineering Research Council of Canada.

**Figure Caption:**

Figure 1. The distribution of nitrogen and boron (black) in the top and bottom triphenylene units and along the equator for isomer 2, and 3.

Figure 2. Geometry of the lowest energy structure of $C_{48}(BN)_6$.

Figure 3. Raman scattering activities of $C_{48}(BN)_6$. Open squares (triangles) and filled circles are fully (incomplete) polarized and unpolarized Raman-active modes, respectively. The solid and dot-dashed lines are the calculated unpolarized and polarized Raman spectral lines of $C_{60}$, respectively (from ref.[12]).

Figure 4. Optical absorption spectra of (a) $C_{60}$ (adapted from ref.[7]) and (b) $C_{48}(BN)_6$ calculated at the TD-BP86/3-21G level. The vertical lines are the calculated oscillator strengths $f_{osc}$ (bottom) and singlet energies (top). Lorentzian function has been used to simulate a finite broadening for the absorption spectrum.

Figure 5. Single-electron energy levels (LUMO+$n$ and HOMO-$n$, $n$ = 0,1,…,9) of $C_{48}(BN)_6$ in its ground state calculated at the BP86/3-2G level. Filled (open) circles denote occupied (unoccupied) molecular orbitals.

**Table I**. Calculated energetic of $C_{48}B_6N_6$ isomers at the B3LYP/6-31G* level.

| Structure | Total energy (hartree) | ΔE [a] (Kcal/mol) |
|---|---|---|
| 1 | -2306.810242 | 0.0 |
| 2 | -2306.562923 | 155.2 |
| 3 | -2306.543870 | 167.2 |
| 4 | -2306.513026 | 186.5 |

[a] ΔE is the relative energy.

Table II. Calculated energetic and electronic properties of $C_{48}(BN)_6$, $C_{48}B_{12}$, $C_{48}N_{12}$, and $C_{60}$.[a]

| **Molecule** | **HOMO (eV)** | **LUMO (eV)** | **IP (eV)** | **Binding Energy** (eV/atom) |
|---|---|---|---|---|
| $C_{48}(BN)_6$ | -5.713 | -2.990 | 6.920 | 6.69 |
| $C_{48}B_{12}$ | -5.688 | -4.084 | 6.872 | 6.62 |
| $C_{48}N_{12}$ | -4.901 | -2.162 | 6.157 | 6.38 |
| $C_{60}$ | -5.986 | -3.225 | 7.240 | 6.98 |

[a] $C_{48}B_{12}$, $C_{48}N_{12}$, and $C_{60}$ calculations are from Ref.[14].

**Table III**. Harmonic vibrational frequencies and IR intensity of $C_{48}(BN)_6$.

| | **Frequencies** |
|---|---|
| **IR active modes** [a] | 343(1), 434(2), 474(2), 481(6), 482(1), 493(8), 510(5), 512(4), 527(14), 530(8), 539(15), 542(4), 544(3), 550(16), 552(14), 559(26), 576(2), 651(2), 654(3), 656(6), 683(2), 687(3), 691(5), 692(6), 698(7), 700(6), 705(8), 709(5), 713(12), 725(1), 731(3), 734(2), 738(2), 744(5), 746(7), 749(3), 754(8), 756(2), 758(2), 761(5), 767(3), 770(1), 772(12), 776(20), 780(1), 784(1), 793(6), 797(3), 805(2), 937(5), 938(9), 946(20), 968(3), 977(3), 979(3), 1072(2), 1079(3), 1081(1), 1088(8), 1093(6), 1114(18), 1121(2), 1132(2), 1146(6), 1152(12), 1170(11), 1173(40), 1175(28), 1190(9), 1201(5), 1207(6), 1211(3), 1226(7), 1230(25), 1234(9), 1238(12), 1262(5), 1273(4), 1281(5), 1285(38), 1285(12), 1294(4), 1305(3), 1307(14), 1314(10), 1320(8), 1327(5), 1330(2), 1338(4), 1339(9), 1343(20), 1345(4), 1350(7), 1357(3), 1363(21), 1370(35), 1374(10), 1375(4), 1382(9), 1391(22), 1395(14), 1397(26), 1402(33), 1412(3), 1418(16), 1419(20), 1428(36), 1437(13), 1450(6), 1464(2), 1532(42), 1539(40), 1542(9), 1545(21), 1550(28), 1557(16), 1560(2), 1567(1), 1581(6), 1583(33), 1585(10), 1595(28), 1599(53), 1600(34), 1604(35), |
| **Non-active modes** | 244, 244, 249, 261, 263, 313, 324, 327, 335, 346, 353, 387, 388, 392, 393, 394, 395, 397, 403, 436, 454, 463, 468, 505, 557, 571, 575, 575, 577, 581, 584, 662, 662, 684, 685, 736, 741, 747, 764, 774, 819, 821, 829, 923, 1005, 1073, 1218, 1261, 1601, |

[a] Frequency in $cm^{-1}$. IR intensities in km/mol are in parenthesis.

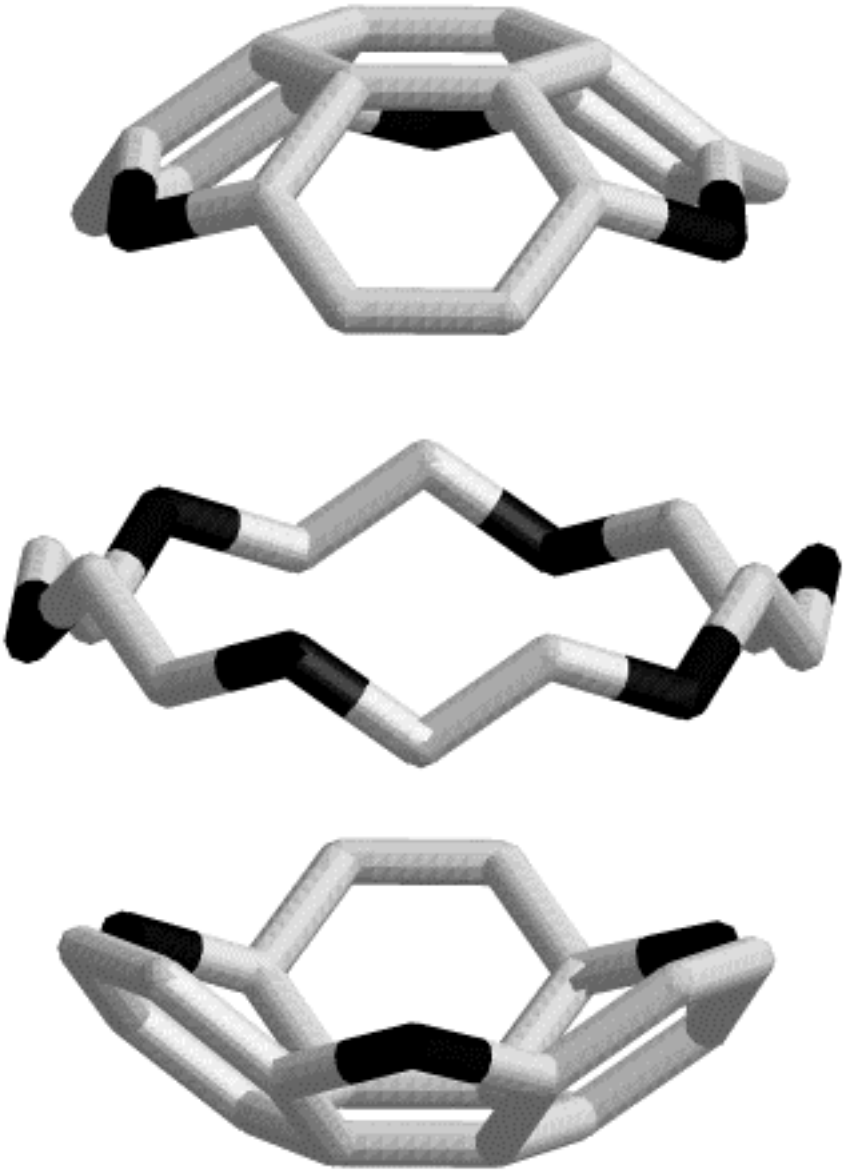

Manaa et al.: Figure 1.

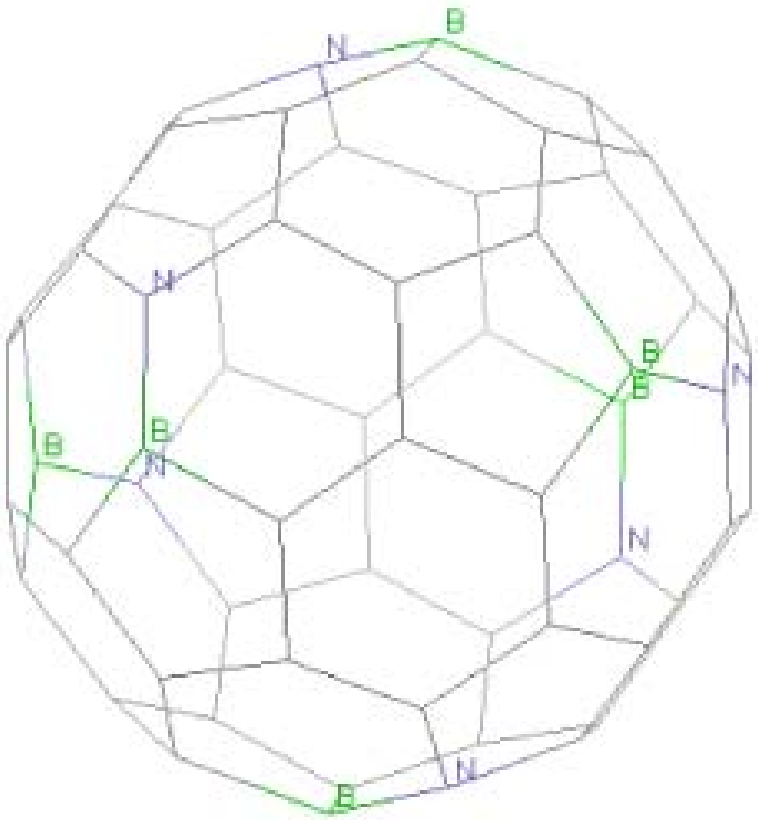


Manaa et al.: Figure 2.

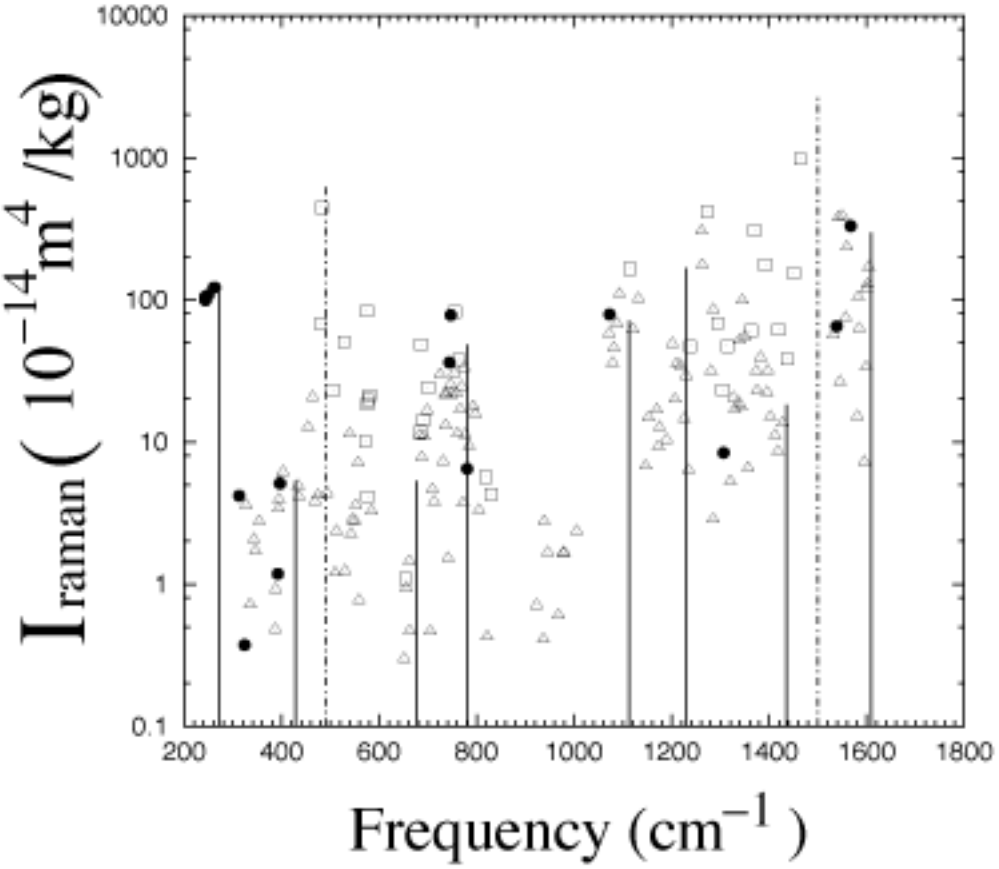


Manaa et al.: Figure 3.

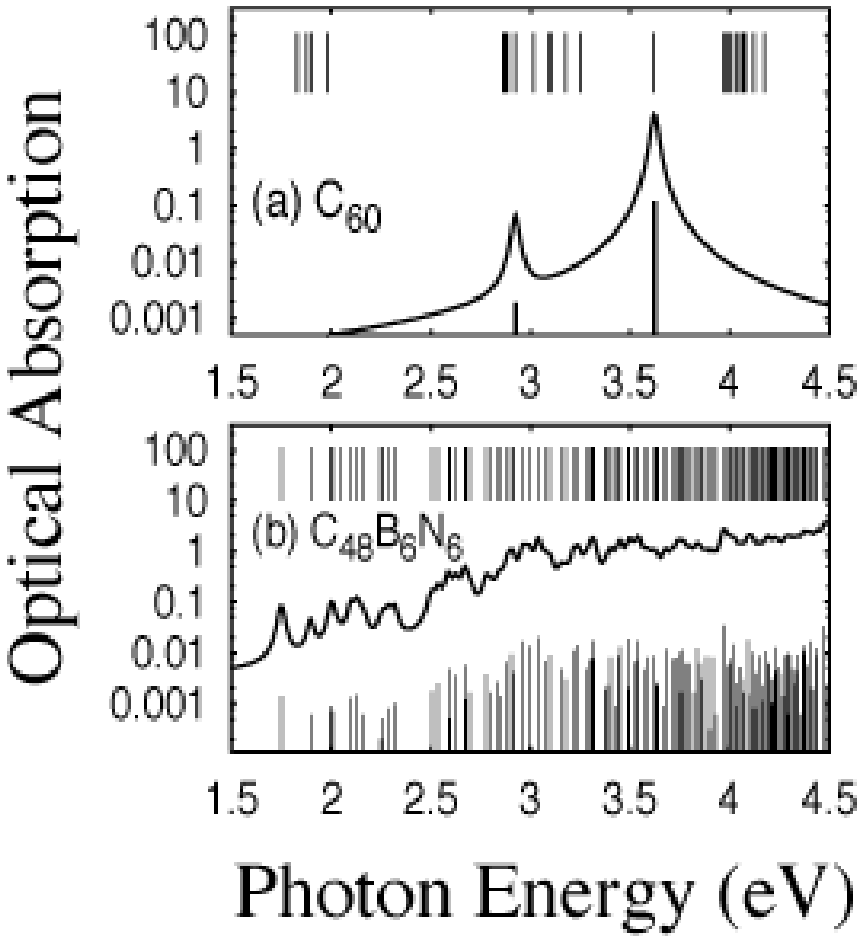


Manaa et al.: Figure 4.

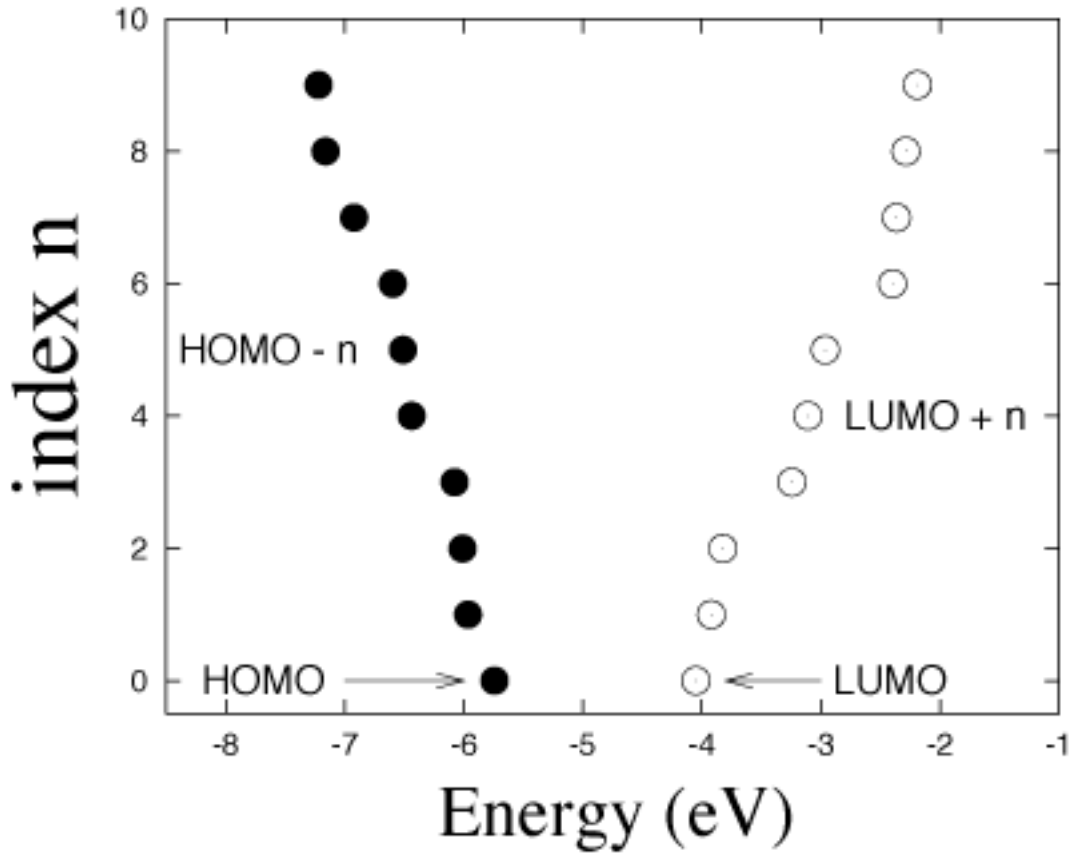


Manaa et al.: Figure 5.

References:


[1] S. Glenis, S. Cooke, X. Chen, and M. N. Labes, Chem. Mater. 6, (1994) 1850.

[2] T. Guo, C. M. Jin, and R. E. Smalley, J. Phys. Chem. 95, (1991) 4948.

[3] L. Hultman, S. Stafstrom, Z. Czigany, J. Neidhardt, N. Hellgren, I. F. Brunell, K. Suenaga, and C. Colliex, Phys. Rev. Lett. 87, (2001) 225503.

[4] M. R. Manaa, D. W. Sprehn, and H. A. Ichord, J. Am. Chem. Soc. 124, (2002) 13990.

[5] M. R. Manaa, D. W. Sprehn, and H. A. Ichord, Chem. Phys. Lett. 374, (2003) 405.

[6] B. Brena and Y. Luo, J. Chem. Phys. 119, (2003) 7139.

[7] R. H. Xie, G. W. Bryant, G. Sun, M. C. Nicklaus, D. Heringer, T. Frauenheim, M. R. Manaa, V. H. Smith Jr., Y. Araki, and O. Ito, J. Chem. Phys. in press (2004).

[8] M. R. Manaa, Solid State Commun. 129, (2004) 379.

[9] S. Stafstrom, L. Hultman, and N. Hellgren, Chem. Phys. Lett. 340, (2001) 227.

[10] R. H. Xie, G. W. Bryant, and V. H. Smith, Chem. Phys. Lett. 368, (2003) 486.

[11] R. H. Xie, G. W. Bryant, L. Jensen, J. Zhao, and V. H. Smith, J. Chem. Phys. 118, (2003) 8621.

[12] R. H. Xie, G. W. Bryant, and V. H. Smith, Phys. Rev. B 67, (2003) 155404.

[13] R. H. Xie, G. W. Bryant, J. Zhao, V. H. Smith, A. D. Carlo, and A. Pecchia, Phys. Rev. Lett. 90, (2003) 206602.

[14] M. R. Manaa, Chem. Phys. Lett. 382, (2003) 194.

[15] J. H. Edgar, J. Mater. Res. 7, (1992) 235.

[16] V. L. Solozhenko, G. Will, H. Hupen, and F. Elf, Solid State Commun. 90, (1994) 65.

[17] A. D. J. Becke, J. Chem. Phys. 98, (1993) 5648.

[18] C. Lee, W. Yang, and R. G. Parr, Phys. Rev. B 37, (1988) 785.

[19] M. R. Manaa, J. Mol. Struct. (Theochem) 549, (2001) 23.

[20] M. R. Manaa, H. A. Ichord, and D. W. Sprehn, Chem. Phys. Lett. 378, (2003) 449.

[21] Z. Chen, H. Jiao, D. Moran, A. Hirsch, W. Thiel, and P. R. Schleyer, J. Phys. Org. Chem. 16, (2003) 726.

[22] J. M. L. Martin, J. El-Yazal, J. P. Francois, and R. Gijbels, Chem. Phys. Lett. 232, (1995) 289.

[23] R. W. Lof, M. A. van Veenendaal, B. Koopmans, H. T. Jonkman, and G. A. Sawatzky, Phys. Rev. Lett. 68, (1992) 3924.

[24] K. Lynch, C. Tanke, F. Menzel, W. Brockner, P. Scharff, and E. Stumpp, J. Phys. Chem. 99, (1995) 7985.